

Hydrogen ordering and metal-semiconductor transitions in the system YH_{2+x}

J. N. Daou and P. Vajda*

Hydrogène dans les métaux, Bâtiment 350, Université Paris-Sud, F-91405 Orsay, France

(Received 25 November 1991)

The electrical resistivity of $\beta\text{-YH}_{2+x}$ specimens, measured between 1.5 and 330 K, exhibits, for $x \geq 0.05$, a break in $d\rho/dT$ centered at 155 K, which is attributed to short-range ordering of the excess-hydrogen atoms on octahedral sites. This anomaly is, for $x \geq 0.085$, superimposed by a first-order transition in the region 200–240 K, probably due to long-range ordering in the H_O sublattice as suggested by the analysis of quenching experiments. Moreover, it appears to be the driving mechanism for a metal-semiconductor (M - S) transition, at 235 and 255 K for $x = 0.10$ in the cooling and in the heating regime, respectively, and at 280 K for $x = 0.095$ when warming up after a quench. At the same time, a resistivity minimum shows up at low temperatures, whose depth and position grow with x increasing from 0.085 to 0.10: from 0.01 to $7.5 \mu\Omega \text{ cm}$ and from 10 to 79 K. The origin of the M - S transition is ascribed to the collapse of a delocalized band near the Fermi energy which forms below the transition temperature due to H_O -atom ordering; that of the low- T transition is tentatively attributed to carrier localization due to hydrogen disorder. We have also determined, by x-ray lattice-parameter measurements, the boundary of the pure β phase to $x_{\beta}^{\text{max}} = 0.10$. This shows that the insulating γ phase coexisting just above $x = x_{\beta}^{\text{max}}$ may also participate in the driving mechanism for the M - S transitions, e.g., as percolating micrograins present at, and just below, x_{β}^{max} .

INTRODUCTION

The superstoichiometric rare-earth dihydrides, $\beta\text{-RH}_{2+x}$, form interesting systems whose structural and electronic properties depend on the concentration of the excess hydrogen atoms x . The latter are localized in the octahedral (O) interstitial sites of the dihydride lattice, which crystallizes in the fcc fluorite-type structure with, ideally, all tetrahedral (T) sites filled up. Thus, the x excess-hydrogen atoms can interact with one another and with the T -site hydrogen atoms, organizing themselves for $x \geq 0.05$ at. % H/at. % R into short-range-ordered structures which turn into long-range order for higher x values, typically above $x \sim 0.15$ at. % H/at. % R (for a review, see, e.g., Ref. 1). This structural order, forming an H_O sublattice, sometimes distorts the metal sublattice from cubic into tetragonal, as in the case of RH_{2+x} with $R = \text{La}$,² Ce ,^{3,4} or Sm ,^{5,6} and has always a striking incidence upon any existing magnetic order, as for $R = \text{Ce}$,^{7,8} Pr ,⁹ Nd ,¹⁰ Sm ,¹¹ Gd ,¹² Tb ,¹³ or Dy .¹⁴ Moreover, metal-semiconductor transitions (when increasing the temperature) had been observed in the x -rich systems CeH_{2+x} ($0.7 \leq x \leq 0.8$) (Refs. 15 and 16) and LaH_{2+x} ($0.8 \leq x \leq 0.9$) (Refs. 16 and 17) as well as incipient ones in $\text{PrH}_{2.76}$ (Ref. 18) and $\text{NdH}_{2.65}$.¹⁰ These transitions occurred in the interval 200–250 K and were attributed to the breaking down of a superlattice of octahedral vacancies, V_O , forming below this temperature range.

Recently, we had started an investigation of the system YH_{2+x} , hoping to obtain unambiguous results from this essentially simple (nonmagnetic) and chemically stable (when compared to the RH_{2+x} compounds with $R = \text{La}$, Ce , Pr , and Nd) dihydride, going down to the liquid-helium temperature range. To our surprise, we had ob-

served a clear metal-semiconductor transition near $T_p = 250$ K for an x value as low as $x = 0.10$ and a second one when decreasing the temperature, near 80 K.¹⁹ We had attributed the former to the breakdown of a superlattice of the octahedral hydrogens, H_O , themselves forming in this *superstoichiometric dihydride*, in contrast to the V_O superlattice in the above-mentioned rather *substoichiometric trihydrides*; the low-temperature transition seemed more of a weak-localization type. In what follows we will present the complete results of this study, showing in particular the evolution of the resistivity behavior with the excess-hydrogen concentration x when approaching the phase boundary towards the hexagonal trihydride (γ phase), the latter being determined by x-ray diffraction.

EXPERIMENT

The specimens were prepared from 99.99 at. % yttrium foil of 200 μm thickness purchased from the Ames Laboratory (Ames, Iowa), which contained as stated main metallic impurities (> 1 at. ppm): 20 Fe, 19 W, 5 Ni, 4 Cu, 3 Al, 3 Pb, and < 2 Hf and the other rare earths 11 La, 3.5 Pr, 3 Ce, 3 Gd, and 2.8 Tb; vacuum fusion analysis gave as the main gaseous contents (in at. ppm): 2000 O, 2500 H, and 60 N. The foils were cut into $20 \times 1 \text{ mm}^2$ strips and provided with four spot-welded platinum leads as contacts. The ensuing hydrogenation took place in two steps: (1) the preparation of the dihydride by direct absorption in a calibrated volume at 550°C – 600°C , resulting in a composition of the “pure” dihydride $\text{YH}_{1.98(1)}$; (2) the addition of the excess concentration x at a temperature of 250°C – 300°C . The concentrations were determined by pressure-difference measurements with a Bara-

tron high-precision capacitance manometer to ± 0.005 at. % H/at. % Y. The finally prepared YH_{2+x} specimens had the following concentrations: $x=0, 0.025, 0.04, 0.05, 0.085, 0.095, 0.10,$ and 0.19 ; a dideuteride, $\text{YD}_{1.97}$ ($x=0$ D), was also prepared, for comparison. [It will be shown later that the $x=0.19$ sample is already situated within the two-phase ($\beta+\gamma$) region.]

The resistivity measurements were done by the dc four-point method in a pumped liquid-helium cryostat in the temperature range $1.5 \leq T \leq 330$ K. Two regimes were applied to study the influence of possible H_O -sublattice ordering: (1) relaxed (R), with the samples slowly cooled from room temperature to liquid nitrogen, with a rate of ~ 0.2 K/min, the measurements being taken both with decreasing and with increasing T ; (2) quenched (Q), with the sample holder dipped into liquid nitrogen at a rate of $\sim 10^3$ K/min. The hydrogen atoms being immobile below ~ 150 K, the subsequent rapid cooling due to liquid-helium transfer did not introduce any additional problems.

X-ray diffraction measurements were performed in a liquid-nitrogen cryostat between 85 and 300 K on most specimens, after the resistivity runs, to determine the temperature dependence of the lattice parameter and the solubility limit of the excess hydrogen atoms in the β phase. The lattice parameter was deduced after treating the positions of twelve lines in the angular region $60^\circ \leq 2\theta \leq 160^\circ$ (Cu $K\alpha$ radiation) by means of a statistical refinement program applying various corrections, to an absolute precision of $\Delta a/a = 2 \times 10^{-4}$ and a relative one of better than 10^{-4} .

RESULTS AND DISCUSSION

Electrical resistivity

In Figs. 1–3, we present the temperature dependence of the electrical resistivity of several selected YH_{2+x} specimens, showing its evolution with increasing x . The pure dihydride, with $x=0$ (Fig. 1) exhibits the classical behavior

$$\rho(T) = \rho_r + \rho_{ph}(T),$$

where the low value for the residual resistivity, $\rho_r = 0.38$ $\mu\Omega$ cm, and the high resistivity ratio, $\rho_{295\text{K}}/\rho_r = 32$, are a sign for the absence of octahedral x atoms within our sensitivity of $\sim 10^{-3}$ at. % H/at. % Y. The slight upturn above ~ 200 K indicates the beginning manifestation of the optical phonons, due to conduction-electron scattering by the vibrations of the (tetrahedral) H_T sublattice. The simultaneously measured dideuteride, $x=0$ D (not shown here), possesses an even smaller residual resistivity, $\rho_r = 0.21$ $\mu\Omega$ cm, with the optical phonons acting already above ~ 150 K because of their lower Einstein temperature. (For a detailed analysis of the optical-phonon–electron coupling, see Ref. 20.) The $x=0.025$ and 0.05 specimens appear just shifted by an added ρ_r . For $x=0.085$ one observes, however, a hysteresis above 200 K and a very shallow (0.01 $\mu\Omega$ cm deep) though definite minimum at 10 K, shown in an enlarged view in

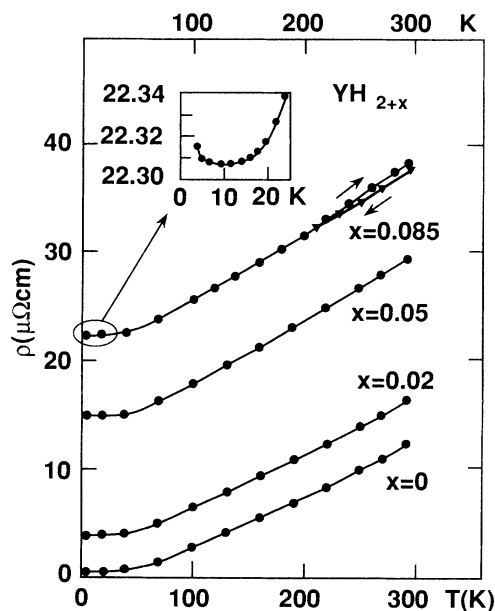


FIG. 1. Electrical resistivity of YH_{2+x} samples, with $x=0, 0.025, 0.05,$ and 0.085 . The $x=0.085$ specimen exhibits a hysteresis above 200 K and a very flat minimum at 10 K (inset).

the inset of Fig. 1.

Adding just 0.01 at. % H/at. % Y, to give $x=0.095$, changes the $\rho(T)$ curve drastically (Fig. 2). The residual resistivity increases to more than 50 $\mu\Omega$ cm, the low- T minimum increases in depth to 1.0 $\mu\Omega$ cm and shifts to

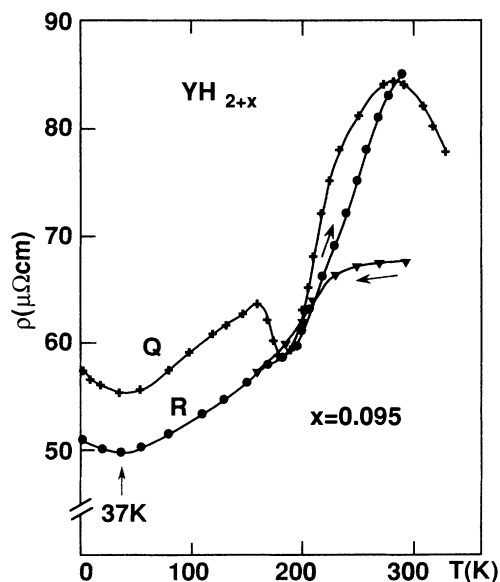


FIG. 2. Electrical resistivity of YH_{2+x} , with $x=0.095$ after slow cooling (R) and after a quench from room temperature (Q). Note the strong hysteresis between the cooling (\blacktriangledown) and heating (\bullet) runs for the R sample and the M - S transition at 280 K for the Q sample. The low- T minimum at 37 K has increased in depth after the quench.

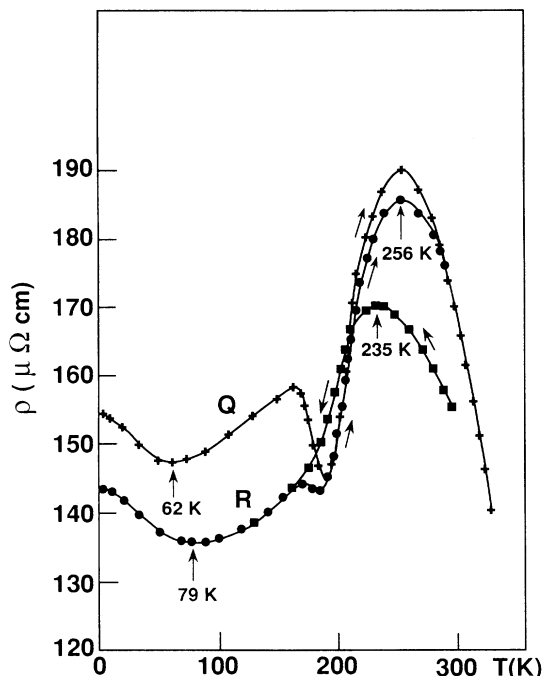


FIG. 3. Electrical resistivity of YH_{2+x} , with $x=0.10$, in the R and Q states. Note the M-S transitions at 235 and 256 K in the cooling (■) and in the heating (●) runs as well as after quench. The low- T minimum has shifted to 60–80 K and increased in depth compared to Fig. 2.

wards 37 K, but, most important, a transition appears near 200 K exhibiting a strong hysteresis effect. It is tempting to attribute this transition, in analogy to other rare-earth hydrides,¹ to a transformation in the hydrogen H_O sublattice, most probably to ordering of the excess-hydrogen atoms. A good test for this hypothesis is a quench across the transition region, which gave the curve labeled Q in Fig. 2. The quench introduced a $\Delta\rho_q=6 \mu\Omega \text{ cm}$, at the same time increasing the depth of the minimum near 40 K to $2.1 \mu\Omega \text{ cm}$. With increasing temperature, the $\Delta\rho_q$ begins to recover at $T=160 \text{ K}$ and has completely annealed out at 190 K. Going even higher in temperature separates the Q and R curves again, the former turning in to a maximum at 284 K. A subsequent heating up to 330 K confirms the metal-to-semiconductor aspect of the transition at 284 K.

Figure 3, which shows the resistivity of the $x=0.10$ specimen and is drawn from Ref. 19, emphasizes all features of the $x=0.095$ sample: ρ_r jumps in the relaxed (R) state to $143 \mu\Omega \text{ cm}$, the position of the minimum shifts to 79 K, its depth increases to $7.5 \mu\Omega \text{ cm}$, and the metal-to-semiconductor transition is present in all cases—with decreasing T at 235 K, with increasing T at 256 K both after slow cooling and after the quench. The latter reduces slightly the temperature of the minimum to 62 K and its depth to $7.0 \mu\Omega \text{ cm}$. It seems clear that the situation of the order-disorder transformation above 200 K, which is supposed¹⁹ to drive the M-S transition, is not very stable, since the quenching treatment modifies the

transition temperature, for $x=0.10$, or even provokes its appearance as in the case of $x=0.095$.

The low-temperature resistivity minimum, which shows up in parallel with the ordering anomaly above 200 K and initiates another M-S transition towards lower temperatures, is possibly related to an electron localization problem by the atomic disorder of hydrogen due to interference processes²¹ that are destroyed at higher temperatures by phonon scattering. The fact that additional disorder introduced by a quenching treatment increases the localization minimum, at least for the $x=0.095$ sample, speaks in favor of the above mechanism, in the same way as its appearance only in samples with appreciable ρ_r . [Though the resistivities involved here are, surprisingly, still an order of magnitude smaller than in the systems NdH_{2+x} (for $x=0.64$ and 0.65) (Ref. 10) and LuH_{2+x} (for $x=0.20$),²² where comparable minima had been observed.] A Kondo effect due to contamination by diluted magnetic impurities can be safely excluded, since no minimum whatsoever has been observed in our lower- x dihydrides of the same origin and containing the same metallic impurities.

Let us now look somewhat closer at the transformation region around 200 K. For this, we have plotted in Fig. 4 the derivatives, $d\rho/dT$, of the resistivities for four samples with $0 \leq x \leq 0.095$. While the pure dihydride ($x=0$) possesses in this region a practically constant slope, with just a slow increase from 200 K on due to beginning optical-phonon scattering, the $x=0.05$ sample exhibits a clear anomaly with a maximum at $T_{\text{an}}^{(1)}=155 \text{ K}$. For the $x=0.085$ sample, this anomaly increases in amplitude

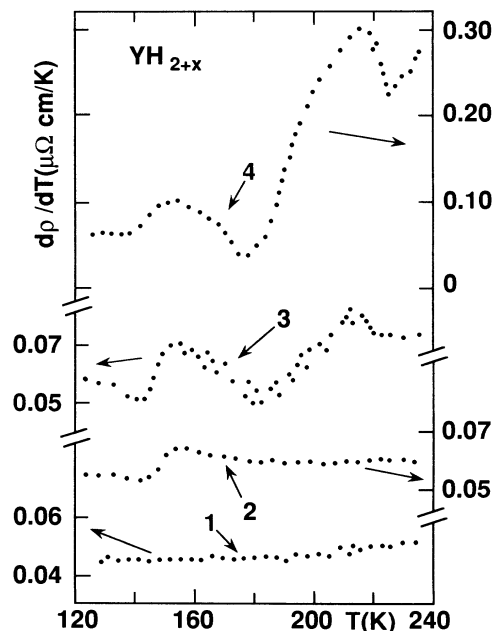


FIG. 4. Resistivity derivatives in the range $120 \leq T \leq 240 \text{ K}$ for YH_{2+x} , with 1, $x=0$; 2, $x=0.05$; 3, $x=0.085$; and 4, $x=0.095$, indicating the appearance of two anomalies centered at 155 and 215 K, respectively. Note the different ordinate scale for sample 4.

and is followed by a second one at $T_{\text{an}}^{(2)}=215$ K. And, finally, in the case of the $x=0.095$ sample, the still appreciable $T_{\text{an}}^{(1)}$ anomaly is overwhelmed by the enormous peak at $T_{\text{an}}^{(2)}$.

It is tempting to attribute the processes responsible for the two anomalies to two ordering mechanisms in the H_O sublattice: (1) that at $T_{\text{an}}^{(1)}$, appearing for $x \gtrsim 0.05$ and predominant at lower x values, to short-range ordering, and (2) that a $T_{\text{an}}^{(2)}$, stable at higher temperatures and predominant for higher x , to long-range ordering. A kinetic analysis of the recovery process of the quench-induced resistivity increase, $\Delta\rho_q$ (cf. Figs. 2 and 3), can provide additional information about the mechanisms involved. Thus, one can determine the activation energy E_m for the migrating hydrogen atom during the recovery process, assuming a first-order single activated mechanism, from

$$E_m = kT_p^2 \frac{d\Delta\rho_q(T_p)/dT}{\Delta\rho_q(T_p)}$$

by measuring the annealed $\Delta\rho_q$ and its derivative at the peak temperature T_p of the process (for details see, e.g., Ref. 23). We have performed such an analysis for the specimens with $x=0.095$ and 0.10 , where the predominance of the ordering process at $T_{\text{an}}^{(2)}$ permits a sufficient separation, and show it in Fig. 5. The peaks centered at $T_p=172.5$ and 180 K, respectively, are very close to Gaussian, except for the high-temperature tails indicating the beginning superposition of a new process, and give activation energies of

$$E_m(x=0.095)=0.35(2) \text{ eV} ,$$

$$E_m(x=0.10)=0.31(2) \text{ eV} .$$

These values are somewhat higher than in other RH_{2+x} systems with comparable x ,^{1,8,18,23} where they were of the order of $E_m \sim 0.25$ eV, but the tendency of having a decreasing E_m with higher x is the same, confirming the early nuclear magnetic resonance measurements on

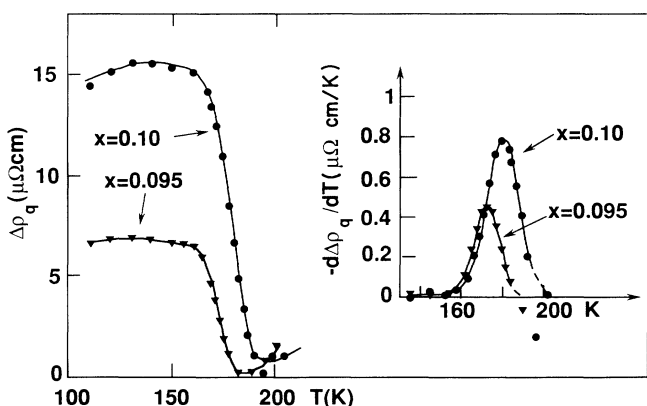


FIG. 5. Thermal annealing of the quenched-in resistivity, $\Delta\rho_q = \rho_Q(T) - \rho_R(T)$, for $x=0.095$ and 0.10 . Inset: derivatives of $\Delta\rho_q$ in the region of the recovery stages at 170 and 180 K, respectively.

LaH_{2+x} (Ref. 24) yielding higher mobility for higher x . This effect could be related, via the higher resistivity, to the decreasing carrier density and increasing ionicity of the samples with higher x , leading apparently to a lower potential barrier for the octahedral jumps.

After having done an analysis of the semiconducting part of the $x=0.10$ specimen in our earlier Letter,¹⁹ we undertake the same treatment on the other sample showing developed M - S transitions, namely, $x=0.095$ (Q) after the quench (see Fig. 2). We present in Fig. 6 the temperature dependence of its electrical resistivity plotted in an Arrhenius graph to deduce an effective activation energy E_a from

$$\rho = \rho_0 \exp(E_a/kT) .$$

The high-temperature part gives

$$E_a = 18 \text{ meV} (\rho_0 = 40 \mu\Omega \text{ cm}) ,$$

which is (within the error limits) the same as the 15 meV deduced for the $x=0.10$ specimen.¹⁹ The low-temperature slope is flatter than that for the latter sample and corresponds to an activation energy of 0.04 meV ($\rho_0 = 55 \mu\Omega \text{ cm}$).

It is obvious that the same phenomenon is taking place in both specimens, and the interplay between the order-disorder transformation and the M - S transition depends very critically on the x concentration. No M - S transition at high T is observed for $x=0.085$ while the ordering anomaly is already clearly present (Figs. 1 and 4), and for $x=0.095$ a quench is necessary to destabilize the H_O sublattice to provoke its collapse and the following M - S transition. An analysis in the framework of variable-range hopping, as suggested by Shinar *et al.*¹⁷ for their x -rich LaH_{2+x} systems, did not give a satisfactory fit in the case of our YH_{2+x} specimens with M - S transition, indicating that it might be rather valid for samples with higher resistivities (or lower carrier densities), with ρ exceeding several $\text{m}\Omega \text{ cm}$. It is also true that the form of

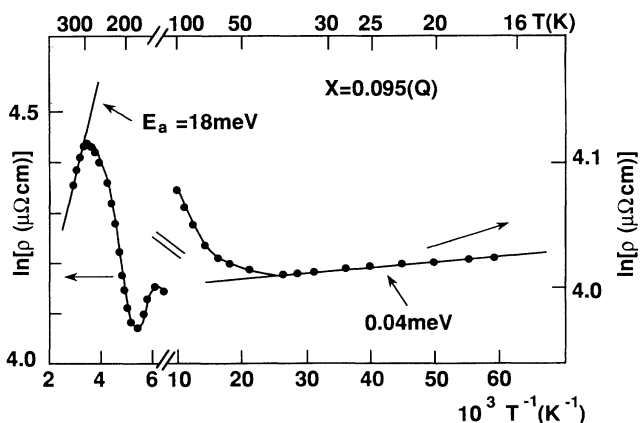


FIG. 6. Arrhenius graph in the high- T (left) and low- T (right) regions for the quenched $x=0.095$ specimen, with the determined effective activation energies as indicated. Note the different ordinate scales.

our $\rho(T)$ curves around the M - S transition more closely resembles those of LaH_{2+x} with lower ρ ($< 1 \text{ m}\Omega \text{ cm}$), such as that of $\text{LaH}_{2.70}$,¹⁶ than those with higher x . (An interesting analogue represents the treatment by Kumar²⁵ of hole movement in an antiferromagnetically correlated matrix, where he finds that isolated holes are localized at discrete energy levels, giving an antiferromagnetic insulator, but that incipient pairing, from certain concentrations on, leads to delocalization with metallic conduction. At intermediate concentrations, however, the long-range order is lost and the system is a semiconductor.)

It is furthermore important, in this context, to consider the resistivity isotherms plotted as a function of x in Fig. 7. The nearly linear dependence of ρ on the hydrogen concentration up to $x=0.085$ diverges suddenly for higher x values, indicating the approach towards insulating behavior, independently of any order-disorder mechanism, as it is equally present for the $\rho_{0 \text{ K}}$ isotherm. It seems obvious that the samples are approaching the phase boundary to the insulating γ phase, which percolates across the metallic dihydride phase giving the stronger than exponential ρ rise and a rather unstable situation of the band structure, the latter "tilting over," in a way, after the collapse of the ordered H_O sublattice. Analogous behavior was observed for the resistivity isotherms in NdH_{2+x} with x approaching $x=0.65$ (Ref. 10) and for GdH_{2+x} close to $x=0.30$.^{12,26} Additional support for the above model can be obtained from an x-ray analysis, the results of which are given in the next section.

Lattice-parameter determination

We have taken x-ray diffraction spectra for most YH_{2+x} specimens employed in the resistivity measure-

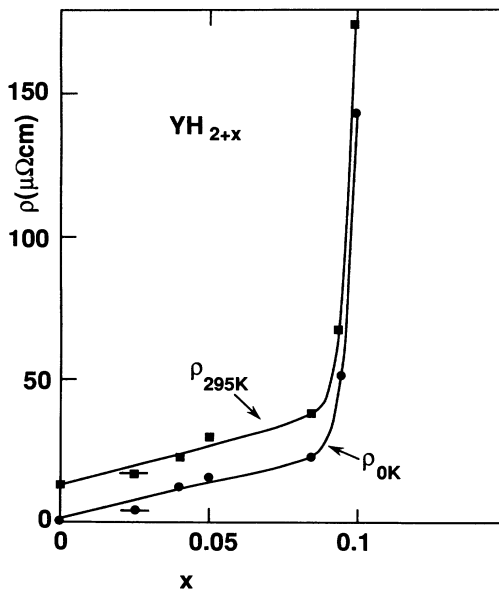


FIG. 7. Resistivity isotherms of YH_{2+x} at 295 and 0 K as a function of the excess hydrogen concentration x . Note the diverging resistivities when approaching $x=0.1$.

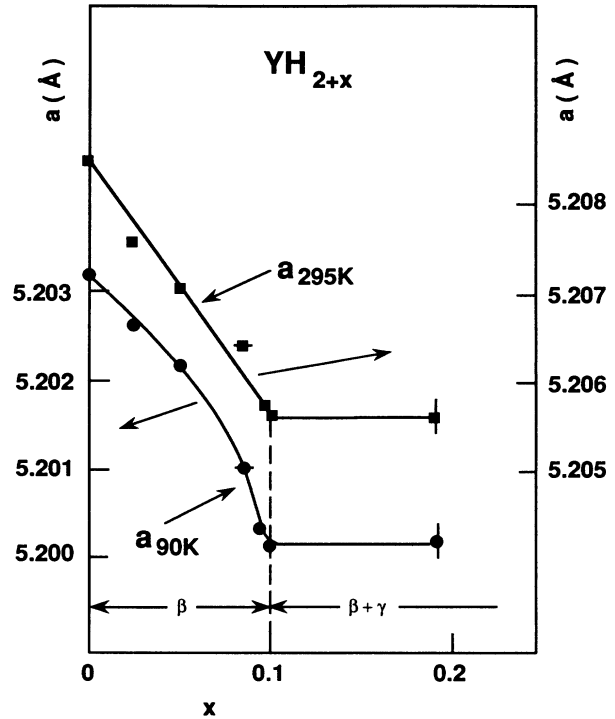


FIG. 8. Lattice parameter of YH_{2+x} as a function of the excess-hydrogen concentration x at 295 and 90 K, indicating the β -phase boundary at $x_{\beta}^{\text{max}}=0.10$.

ments and have determined their lattice parameters as a function of temperature between liquid-nitrogen and room temperatures. Figure 8 shows two isotherms resulting from the above experiments as a function of the x concentration. (The numerical data have been collected in Table I.) Two interesting observations can be noted: (i) the lattice contraction with increasing x (due to increasing ionicity; see Ref. 27, for example) is linear at room temperature, with a coefficient $\beta=(1/a)\Delta a/\Delta x = -0.55 \times 10^{-2}$ per atom H, but superlinear at 90 K; (ii) no further contraction is observed above $x=0.10$.

The first point seems to be a good reflection of the H_O sublattice ordering below room temperature, effective above $x \sim 0.05$, and leading apparently to an additional diminution of the lattice constant. A similar phenomenon has been observed by us earlier on the system SmH_{2+x} ,²⁸ though the specific contraction β had been twice as large there because of the more open lattice. The second point, a contraction limit at $x=0.10$, is

TABLE I. Lattice parameters in the β - YH_{2+x} system.

x (at. % H/at. % Y)	$a_{295 \text{ K}}$ (\AA)	$a_{90 \text{ K}}$ (\AA)
0	5.2085(3)	5.2032(3)
0.025	5.2076	5.2026
0.05	5.2071	5.2022
0.085	5.2064	5.2011
0.095	5.2057	5.2003
0.10	5.2056	5.2002
0.19	5.2056	5.2002

a clear indication that we have reached the phase boundary of the pure β phase; incidentally, the $x=0.19$ specimen had decomposed in air rapidly showing the presence of the very unstable γ phase. The fact that the phase limit is the same for both low- and high- T isotherms is an argument against a possible precipitation of γ -phase regions below room temperature as explanation for the 200–250-K anomaly; in that case, x_{β}^{\max} should have been lower at 90 K.

The above results are, however, also a further indication for an eventual implication of the insulating γ phase in the M - S transitions observed. It is probable that the presence of microscopic γ -phase nuclei in the β -phase matrix close to the phase boundary, which are also in part supposed to be responsible for the low- T localization minimum, acts in conjunction with the order-disorder transformation to drive the M - S transition. It is even possible that the long-range order-configuration of the H_O sublattice, whose structure in YH_{2+x} remains to be determined but which could be similar to the tetragonally distorted ones observed in other systems,^{2–6} somehow prepares the hexagonal γ phase, in analogy to the ordered-pair configurations in several hcp α -phase systems preparing the fcc β phase (for a review, see, e.g., Ref. 29). The surprising result, however, remains the very low value of x (and also of the resistivity) at which the M - S transitions take place in YH_{2+x} compared to the other rare-earth hydrides.

CONCLUSION

We have observed, in the system β - YH_{2+x} , metal-semiconductor transitions for values of the excess-hydrogen concentration on octahedral sites, $x=0.095$ and 0.10. These transitions take place in the region 230–280 K and are driven by simultaneously occurring

order-disorder transformations between 200 and 250 K in the octahedral H_O sublattice. The microscopic origin of the M - S transitions is supposed to be the breaking up of a delocalized band at the Fermi level leading to localized defect levels, caused by the collapse of the ordered H_O sublattice with increasing temperature. At the same time, the fact that the β -phase limit is determined to be $x_{\beta}^{\max}=0.10$, strongly implies an eventual role of the insulating γ phase, which coexists just above $x=0.10$, in the preparation of the M - S transitions. It seems as if two factors are simultaneously needed for the manifestation of the M - S transition: (i) an order-disorder transformation in the H_O sublattice and (ii) a significant decrease of the carrier concentration. Thus, the absence of point (i) due to early γ precipitation is the reason for the lack of a M - S transition in LuH_{2+x} ,²² in spite of very high ρ values; on the contrary, the systems LaH_{2+x} and CeH_{2+x} do exhibit M - S transitions,^{15–17} despite a continuous β -phase region up to $x=1$, because of the action of point (ii) for high x values. In the intermediate cases, such as in $GdH_{2.30}$ (Ref. 26) and $NdH_{2.65}$,¹⁰ and as for the $YH_{2.10}$ discussed here, point (ii) is manifested by a resistivity diverging at the approach to the phase boundary of the insulating γ phase.

A resistivity minimum observed at low temperatures in specimens with $x \geq 0.085$ is attributed to carrier localization by the atomic disorder of hydrogen. The role of the latter is clearly seen through the influence of a quenching treatment from room temperature across the ordering interval, increasing the low- T minimum and provoking the high- T M - S transition in the $x=0.095$ specimen.

ACKNOWLEDGMENTS

Hydrogène dans les Métaux is part of the Laboratoire de Spectroscopie Atomique et Ionique du CNRS.

*Also at Laboratoire des Solides Irradiés, Ecole Polytechnique, F-91128 Palaiseau, France.

¹P. Vajda, J. N. Daou, and J. P. Burger, *Z. Phys. Chem. NF* **163**, 637 (1989).

²P. Klavins, R. N. Shelton, R. G. Barnes, and B. J. Beaudry, *Phys. Rev. B* **29**, 5349 (1984).

³J. Schefer, P. Fischer, W. Hälg, J. Osterwalder, L. Schlapbach, and J. D. Jörgensen, *J. Phys. C* **17**, 1575 (1984).

⁴E. Borocho and E. Kaldis, *Z. Phys. Chem. NF* **163**, 117 (1989).

⁵O. Greis, P. Knappe, and H. Müller, *J. Solid State Chem.* **39**, 49 (1981).

⁶O. J. Zogal and P. l'Héritier, *J. Less-Common Met.* **177**, 83 (1991).

⁷P. Vajda, J. P. Burger, and J. N. Daou, *Europhys. Lett.* **11**, 567 (1990).

⁸J. P. Burger, P. Vajda, and J. N. Daou, *J. Phys. Chem. Sol.* **52**, 779 (1991).

⁹J. N. Daou, J. P. Burger, and P. Vajda, *Phys. Status Solidi B* **154**, 321 (1989).

¹⁰J. N. Daou, J. P. Burger, and P. Vajda, *Philos. Mag. B* **65**, 127 (1992).

¹¹P. Vajda, J. N. Daou, and J. P. Burger, *Phys. Rev. B* **40**, 500

(1989).

¹²P. Vajda, J. N. Daou, and J. P. Burger, *J. Less-Common Met.* **172-174**, 271 (1991).

¹³P. Vajda, J. N. Daou, and J. P. Burger, *Phys. Rev. B* **36**, 8669 (1987).

¹⁴P. Vajda and J. N. Daou, *Phys. Rev. B* **45**, 9749 (1992).

¹⁵G. G. Libowitz, J. G. Pack, and W. P. Binnie, *Phys. Rev. B* **6**, 4540 (1972).

¹⁶J. Shinar, B. Dehner, B. J. Beaudry, and D. T. Peterson, *Phys. Rev. B* **37**, 2066 (1988).

¹⁷J. Shinar, B. Dehner, R. G. Barnes, and B. J. Beaudry, *Phys. Rev. Lett.* **64**, 563 (1990).

¹⁸J. P. Burger, J. N. Daou, and P. Vajda, *Philos. Mag. B* **58**, 349 (1988).

¹⁹P. Vajda and J. N. Daou, *Phys. Rev. Lett.* **66**, 3176 (1991).

²⁰J. N. Daou, A. Lucasson, P. Vajda, and J. P. Burger, *J. Phys. F* **14**, 2983 (1984).

²¹P. A. Lee and T. V. Ramakrishnan, *Rev. Mod. Phys.* **57**, 287 (1985).

²²J. N. Daou, P. Vajda, J. P. Burger, and D. Shaltiel, *Europhys. Lett.* **6**, 647 (1988); **8**, 587 (1989).

²³J. N. Daou, P. Vajda, J. P. Burger, and A. Lucasson, *Phys.*

- Status Solidi A **98**, 183 (1986).
- ²⁴D. S. Schreiber and R. M. Cotts, Phys. Rev. **131**, 1118 (1963).
- ²⁵N. Kumar, Phys. Rev. B **42**, 6138 (1990).
- ²⁶P. Vajda and J. N. Daou (unpublished).
- ²⁷A. Pebler and W. E. Wallace, J. Phys. Chem. **66**, 148 (1962).
- ²⁸J. N. Daou, P. Vajda, and J. P. Burger, Solid State Commun. **71**, 1145 (1989).
- ²⁹J. N. Daou and P. Vajda, Ann. Chim. (Paris) **13**, 567 (1988).